

# Electromagnetic Transients of a Sagging Conductor above Lossy Earth—Effect of its Loading and of the Earth Parameters

*Mohamed M. Saied\**

Professor and Independent Researcher, Giza, Cairo, Egypt

## *Abstract*

*This paper addresses the electromagnetic transients of a non-uniform overhead transmission line conductor with due consideration of its receiving-end load, its sag and of the earth parameters. The concept of the complex penetration depth is adopted in the formulation of the line's equations in the  $s$ -domain. A relation for the conductor height as a function of the longitudinal co-ordinate is derived and incorporated in the analysis. The two simultaneous differential equations governing the voltage and current are solved analytically in order to get closed-form  $s$ -domain expressions for their distributions. The application of numerical Laplace inversion will then yield the distributions in the time domain. Results of different case studies are presented and discussed. The paper is then concluded by validating the proposed technique by discussing the results of its application to a case study of a known analytical solution.*

**Keywords:** *Transmission lines, Laplace transform, non-uniform, electromagnetic transient analysis, earth, numerical analysis*

\**Author for Correspondence* E-mail: m.saied@ieee.org

## INTRODUCTION

The transient analysis of the power transmission elements in general and of the non-uniform overhead lines in particular, was the main topic of several publications [1–15]. An interesting example is the transient performance of sagging overhead lines. The conductor height above ground, which can be also of an uneven terrain, will then be a function of the longitudinal co-ordinate of the points under consideration. Special situations such as river crossings comprising wide span towers were addressed by Saied [13]. Lines with exponentially varying parameters constitute another important category of non-uniformity, for which results of interesting case studies are documented by Nguyen et al. and Saied [7, 8]. In addition to approaches based on circuit theory, several investigators could develop solutions based on the method of characteristics of the lines' partial differential equations [5].

The time-domain analysis by Theethayi et al. [6] deals with the lightning performance of multi-conductor railway lines as affected by

the conductors' heights and the losses in the earth. Martins et al. [9] addresses the accuracy of evaluating the line's internal conductor and earth return impedances. The paper also suggests approximate impedance formulae and their impact on the line's time domain transient response. The interesting concept of the frequency dependent complex penetration depth and its efficient application to the transients of lines involving earth return is presented by Deri et al. [10]. The paper focuses mainly on the longitudinal impedance. Its relation to the Carson's formulae is also pointed out and discussed. Several statements have been made by Moura [11] aiming at improving the modeling of overhead lines when investigating high frequency atmospheric overvoltages. One of the important conclusions is that neglecting the effect of the earth on the line's shunt elements is an acceptable approximation for the usual values of earth conductivity. This also agrees with the related comments made by Gutierrez et al. [5] addressing the effect of frequency and treats the earth as a dispersive medium. Antonescu and Munteanu [12] present the

computed results of case studies involving several shapes of exciting impulse voltages. They demonstrate the impact of the source voltage wave shape, the tower type and the conductors' data on the resulting transients along the sagging lines.

This paper is a contribution to this area of research and has the following main objectives:

1. To suggest an alternative direct method for analyzing the electromagnetic transients in sagging loaded overhead lines above lossy earth. The derived model will take into account the losses dissipated in the line's series and shunt elements and in the earth return. The frequency dependence of the earth return will be also included.
2. To present and discuss the results of several case studies investigating the effect of the receiving-end termination, the line and earth parameters as well as the number of tower spans on the transient response. The results will be given in terms of both the time and the co-ordinate along the line.

**METHOD OF ANALYSIS**

**Geometrical Considerations**

Figure 1 depicts one span length  $d$  of a typical overhead line conductor. The minimum and maximum conductor heights are denoted  $H_{min}$  and  $H_{max}$ , respectively. The per unit conductor sag is defined as  $S = (H_{max} - H_{min}) / H_{max}$ . If the

conductor centenary is approximated by a parabolic expression, the following equation describes the conductor height  $H(x)$  as a function of the horizontal co-ordinate  $x$ , measured from the centerline of the left tower:

$$H(x) = H_{max} \left[ 1 - S + S \left( 1 - \frac{2x}{d} \right)^2 \right] \tag{1}$$

The corresponding expression for a line having  $N$  tower spans is then given by

$$H(x) = H_{max} \left[ 1 - S + S \left( 1 - \frac{2x}{d} \right)^2 \right] [u(x) - u(x-d)] + H_{max} \left[ 1 - S + S \left( 1 - \frac{2[x-d]}{d} \right)^2 \right] [u(x-d) - u(x-2d)] + H_{max} \left[ 1 - S + S \left( 1 - \frac{2[x-2d]}{d} \right)^2 \right] [u(x-2d) - u(x-3d)] + H_{max} \left[ 1 - S + S \left( 1 - \frac{2[x-3d]}{d} \right)^2 \right] [u(x-3d) - u(x-4d)] + \dots$$

+, or, equivalently with the number of tower spans  $N$  included,

$$H(x, N) = \sum_{i=1}^N H_{max} \left[ 1 - S + S \left( 1 - \frac{2[x-[i-1]d]}{d} \right)^2 \right] [u(x-[i-1]d) - u(x-i.d)] \tag{2}$$

where,  $u(x)$  is the unit-step function. Eq. (2) is valid over the region  $0 \leq x \leq N.d$ . As an example, Figure 2 depicts the function  $H(x, 5)$  representing five span lengths.

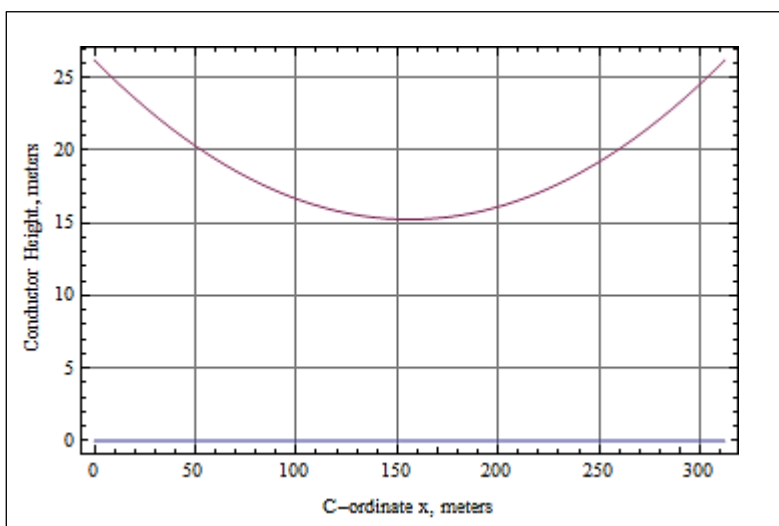


Fig. 1: One span Length of the Overhead Line. ( $d = 329.2m$ ,  $H_{min} = 15.24 m$ ,  $H_{max} = 26.2 m$ ).

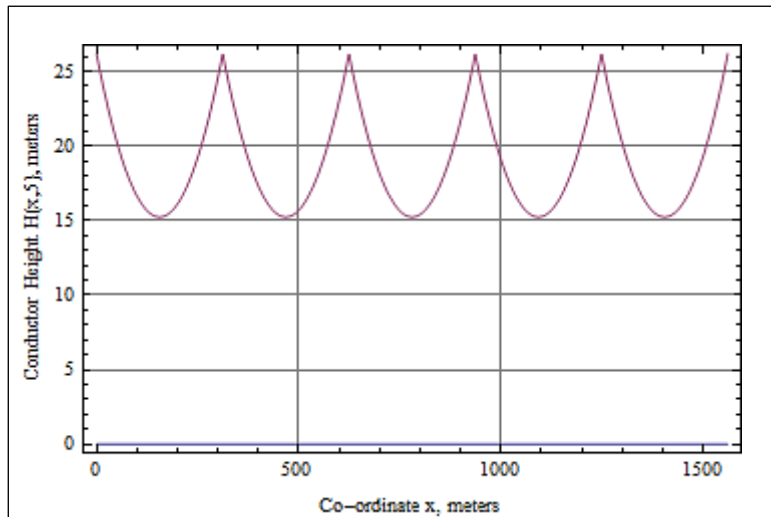


Fig. 2: The Conductor Height for Five Span Lengths, According to Eq. (2) for  $H(x,5)$ .

### The Line's Simulation

After including the effect of the earth return according to the detailed derivations by Thrimawithana and Madawala [2], the series impedance  $z_{series}$  per meter can then be expressed as

$$z_{series}(s,x,N) = r_{earth} + \left(\frac{k r_{dc}}{2}\right) \frac{I_0(k\sqrt{s})}{I_1(k\sqrt{s})} \sqrt{s+s} \frac{\mu_0}{2\pi} \ln\left[\frac{2[H(x,N)+p(s)]}{radius}\right] \quad (3)$$

Where,  $r_{earth}$  and  $r_{dc}$  are the return path resistance and the conductor's DC resistance in  $\Omega/m$ , respectively. The term  $k$  is defined by  $k = radius \sqrt{\mu_0 \sigma}$ .

Eq. (3) indicates that  $z_{series}(s,x,N)$  is composed of three components: the internal conductor impedance due to the internal magnetic fields, the external impedance originating from the magnetic flux outside the conductor and the return path impedance [2].

The two terms  $I_0(k\sqrt{s}), I_1(k\sqrt{s})$  are the modified Bessel functions of the first kind.

Furthermore, the shunt admittance per meter is given by

$$y_{shunt}(s,x,N) = g + s \frac{4\pi\epsilon_0}{\ln\left[\frac{2[H(x,N)]}{radius}\right]} \quad (4)$$

Where,  $g$  is the shunt conductance in  $(\Omega.m)^{-1}$ .

$s$  is the Laplace operator

$\mu_0, \epsilon_0$  are the permittivity and permeability of free space

$radius$  is the conductor radius

$p(s)$  is the complex penetration depth, defined as  $p(s) = 1/\sqrt{s\sigma\mu_0}$ .

In which  $\sigma$  denotes the earth conductivity.

The line's simultaneous differential equations are therefore,

$$\frac{dV(s,x,N)}{dx} = -I(s,x,N) \cdot z_{series}(s,x,N) \quad (5)$$

$$\frac{dI(s,x,N)}{dx} = -V(s,x,N) \cdot y_{shunt}(s,x,N) \quad (6)$$

The boundary conditions are  $V(s,0,N) = E(s)$  at the sending end ( $x=0$ ) and

$\frac{V(s,N,d,N)}{I(s,N,d,N)} = Z_{load}(s)$  at the receiving end ( $x=N.d$ ).

$E(s)$  denotes the Laplace transform of the source voltage  $e(t)$ .

### The Solution Technique

The solution is based on dividing the total line length ( $N.d$ ) into a large number ( $K$ ) of sections of equal lengths  $b = \frac{N.d}{K}$  each. They will not be identical because the conductor height and, accordingly, its circuit parameters per unit length are functions of the co-ordinate  $x$ . The voltages at any two consecutive nodes  $V_k(s,N), V_{k+1}(s,N)$  and the corresponding currents  $I_k(s,N), I_{k+1}(s,N)$  at the beginning and end of the branch connecting them are related by the equations:

$$V_{k+1}(s,N) = V_k(s,N) - I_k(s,N) z_{series}(s, [k+0.5].b, N) \quad (7)$$

$$I_{k+1}(s,N) = I_k(s,N) - V_k(s,N) y_{shunt}(s, [k+0.5].b, N) \quad (8)$$

The above equations indicate that the impedance value  $Z_{seies}$  at the midpoint of the connecting branch is used for computing the voltage drop, while the admittance value  $y_{shunt}$  at the midpoint is substituted for finding the change in the longitudinal current. A sufficient number of equations will be available in order to get closed-form analytical s-domain expressions for all the node voltages and branch currents using the Mathematica command Solve.

The resulting expressions will include:

- i. the Laplace operator  $s$ ,
- ii. the location along the line  $x$ ,
- iii. the span length  $d$ ,
- iv. the number of line's tower spans  $N$ ,
- v. the line constants ( $r_{dc}$ ,  $g$ ,  $radius$ ),
- vi. the minimum and maximum conductor heights ( $H_{min}$ ,  $H_{max}$ ).
- vii. the earth conductivity  $\sigma$ .

Applying the numerical inverse Laplace transform according to Hosono's algorithm [16], the time response of the different voltages and currents along the line can be obtained.

According to the Hosono algorithm, the time function  $f(t)$  corresponding to  $F(s)$  is given by

$$f(t) \approx \frac{e^a}{t} \left[ \sum_{n=1}^{l-1} F_n + \frac{1}{2^{m+1}} \sum_{n=0}^m A_{mn} F_{l+n} \right] \quad (9)$$

where

$$F_n = (-1)^n \text{Im} \left[ F \left[ a + \frac{j(n-0.5)\pi}{t} \right] \right] \quad (10)$$

and

$$a \gg 1, A_{mn-1} = A_{mn} \frac{m+1}{n} + \binom{m+1}{n} \quad (11)$$

In this study the value  $a = 5$  has been assumed. More details are available by Saied [8,13] and Hosono [16].

As will be shown, the presented procedure can handle situations where the line constants and/or the earth conductivity  $\sigma$  are non-

uniformly distributed, i.e., functions of the coordinate  $x$ .

## SAMPLE RESULTS

### The Network Data

The following results refer to a single phase, one single ASCR horizontally suspended conductor of a 2 inch diameter. The earth conductivity is assumed  $\sigma = 0.01(\Omega.m)^{-1}$ , the span  $d = 329.2$  m. The conductor heights are  $H_{min} = 15.24$  m and  $H_{max} = 26.2$  m. The shunt conductance is  $g = 0.01(\Omega.m)^{-1}$ .

In general, a source voltage having a unit-step wave form is assumed. In one of the case studies, however, the voltage waveform depicted in Figure 3 will be considered. It has been used by several investigators, as a test function, and is defined by the following equation:

$$e(t) = 1 - e^{-4545450 t} \quad (12)$$

Where,  $t$  is the time in seconds.

Its Laplace transform is

$$E(s) = \frac{1}{s} - \frac{1}{s+4545450} \quad (13)$$

The following results will describe the time response of the line's receiving-end as well as the voltage distribution along the conductor at specific points in time.

### Transients of a Resistively Loaded Line

Figure 4 illustrates the transient response of the voltage at the line's receiving end which is terminated by each of the indicated three resistance values  $R$ . The time range is  $0 \leq t \leq 10 \mu s$ . The curve on the top shows the step response for the no-load case, i.e.,  $R = \infty$ . It increases very rapidly from zero to a per unit values very close to one. The lower curve is for the smaller load resistance  $R = 1000 \Omega$ . The voltage needs a relatively longer time in order to approach a final value slightly below 1 per unit. The same trend is valid for the smallest load resistance  $R = 100 \Omega$  described by the lowest trace. It indicates a voltage value of 0.9812 per unit at  $t = 10 \mu s$ .

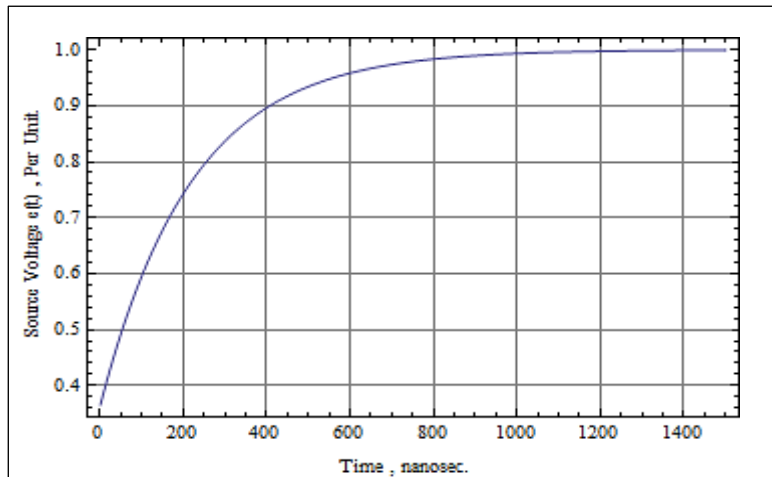


**Fig. 3:** One of the assumed Wave Shapes of the Source Voltage  $e(t)$  over the Time Range  $0 \leq t \leq 1.5 \mu s$  as described by Eq. (10).

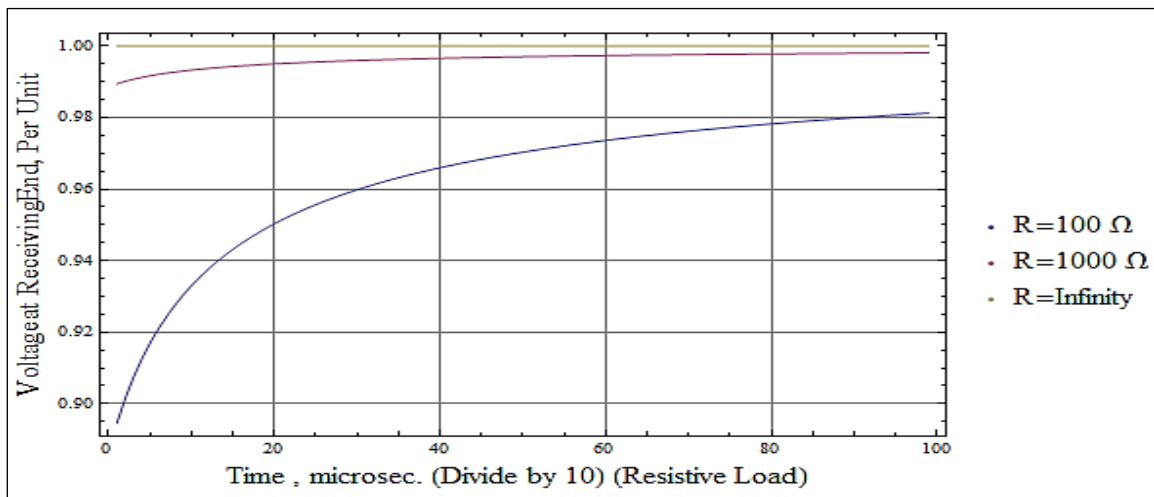


**Fig. 4:** The Transient Response of the Receiving End Voltages for Three Resistive Loading Conditions. The Source Voltage is  $e(t) = u(t)$ .  $g = 0.01$ ,  $\sigma = 0.01(\Omega \cdot m)^{-1}$ .

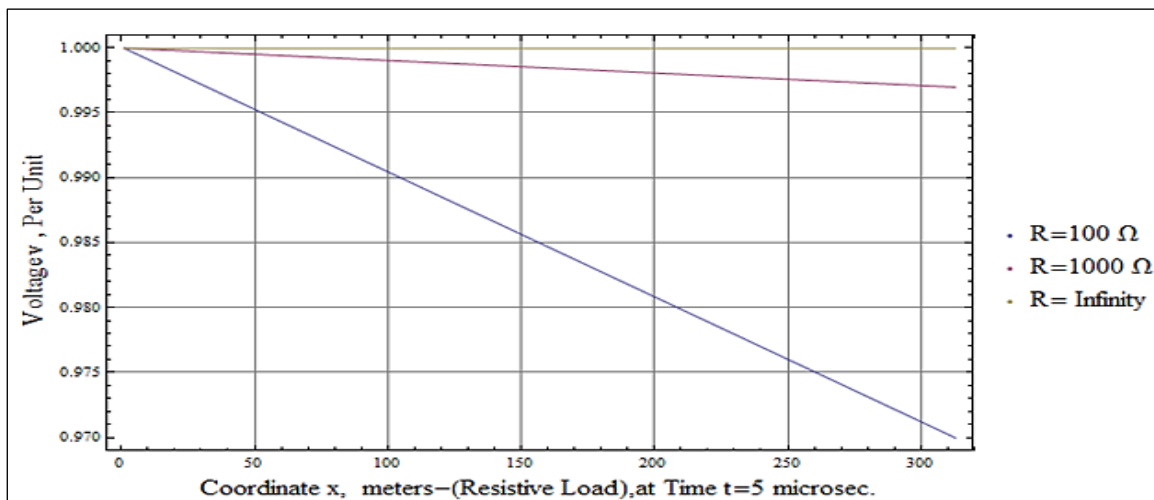


**Fig. 5:** The Distribution of the Transient Voltage along the Line at  $t = 5 \mu s$ .

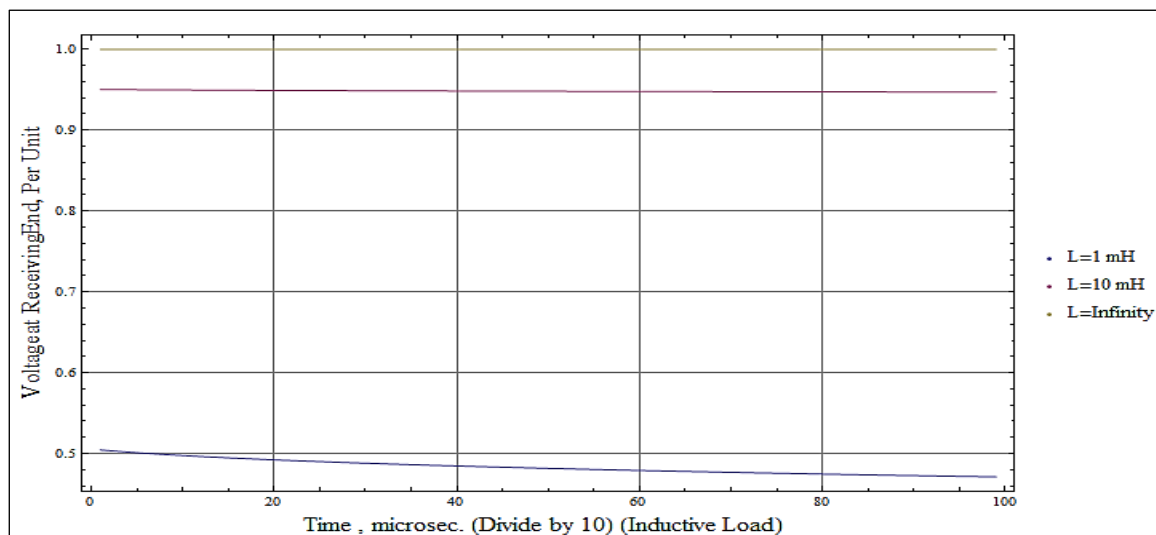


**Fig. 6:** The Transient Response of the Receiving End Voltages for Three Values of the Line's Termination Inductances.  $g = 0.01$ ,  $\sigma = 0.01(\Omega.m)^{-1}$ . The Source Voltage is  $e(t) = u(t)$ .

The distributions of the instantaneous voltage along the transmission line for the three loading conditions at the time point  $t = 5 \mu s$  are depicted in Figure 5. The three curves are almost linear. They start with a voltage value of 1 per unit at the source ( $x = 0$ ). The receiving end voltages at this point in time increase to values ranging from about 0.970 per unit for  $R = 100 \Omega$  to approximately 1.00 per unit at no load.

#### Transients of an Inductively Loaded Line

The instantaneous voltages at the receiving end are illustrated in Figure 6 for the indicated three values of a purely inductive load. The almost flat horizontal curve corresponding to the load inductance  $L = \infty$  is identical to the one describing the no load condition in Figure 4, as expected. At  $t = 10 \mu s$ , the almost linearly decreasing voltages for  $L = 1 \text{ mH}$  and  $L = 10 \text{ mH}$  drop to the approximate values 0.47 and 0.945 per unit, respectively.

A snap shot of the voltage distributions along the line, at the time point  $t = 5 \mu s$ , is given in Figure 7. The voltages decrease almost linearly with the co-ordinate  $x$ , and drop to about 0.946 and 0.475 per unit for the load inductances  $L = 10$  and  $1 \text{ mH}$ , respectively.

These voltages agree with the corresponding values in Figure 6 at  $t = 5 \mu s$ .

#### Transients of a Capacitively Loaded Line

The three load capacitance values  $C = 0$  (i.e., no load),  $C = 0.1 \text{ nF}$  and  $C = 0.2 \text{ nF}$  will be considered in this section. The source voltage  $e(t)$  and its Laplace transform  $E(s)$  are as given by Eqs. (10) and (11). The computation results for the receiving end voltage are depicted in Figure 8. Following the initial rapid changes immediately after the application of the voltage source, the three voltages will gradually approach the (almost equal) final values very close to 1.00 per unit. Beyond  $t = 1 \mu s$ , there is not much difference between the three curves. A voltage overshoot of about 82% is noticed if the load capacitance is  $0.2 \text{ nF}$ . As for the voltage distribution along the line at the time point  $t = 0.5 \mu s$ , the results in Figure 9 indicate that the voltages increase almost linearly with the distance  $x$  measured from the supply point. The rate of voltage rise per unit length increases with the value of the load capacitance. The voltage increase over the entire line assumes the small values of approximately 0, 0.11 and 0.22 per unit for the load capacitances  $C = 0 \text{ nF}$ ,  $C = 0.1 \text{ nF}$  and  $C = 0.2 \text{ nF}$ , respectively.

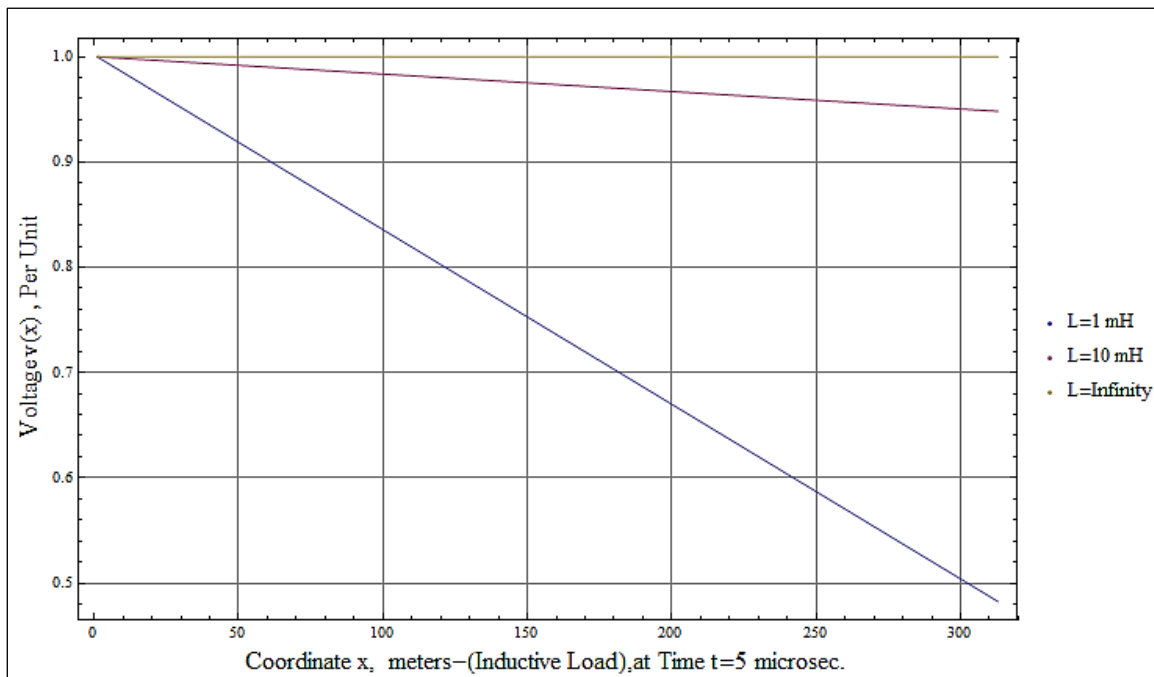


**Fig. 7:** The Instantaneous Voltage versus the Co-ordinate  $x$  at  $t = 5 \mu s$ .

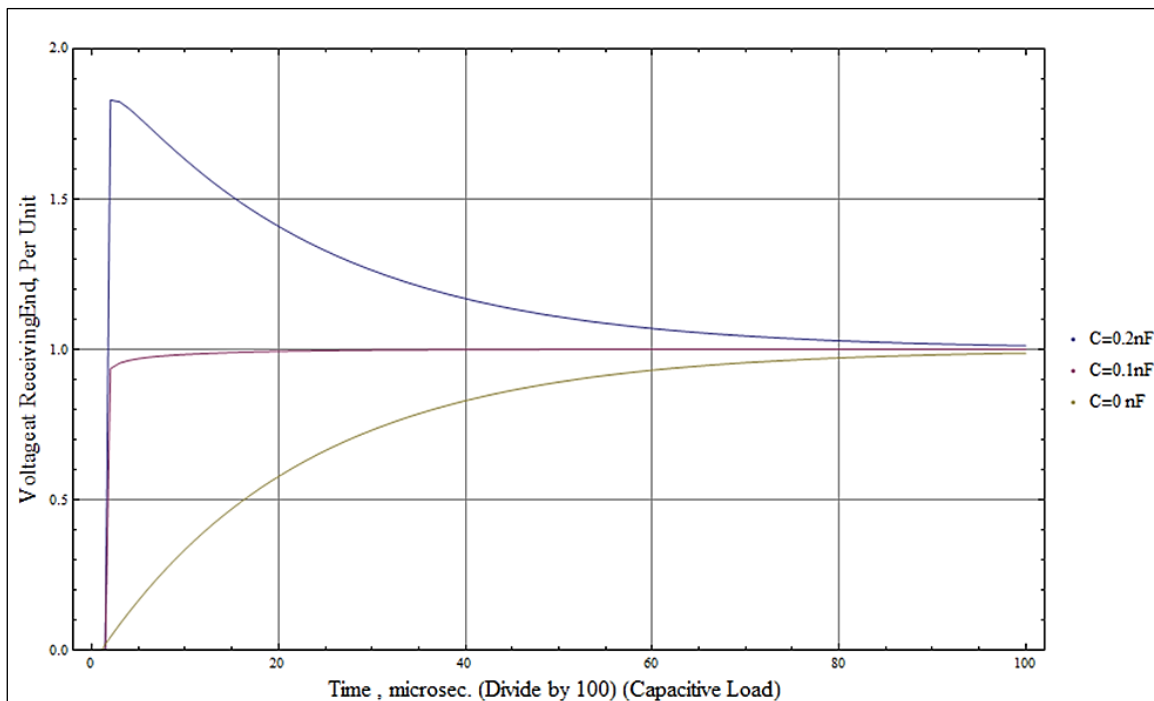


**Fig. 8:** The Transient Response of the Receiving End Voltages for Three Capacitive Loading Conditions. The Source Voltage  $e(t)$  is given by Eq. (10).  
 Lowest curve: Load capacitance  $C = 0 \text{ nF}$ ,  
 Middle curve: Load capacitance  $C = 0.1 \text{ nF}$ ,  
 Upper curve: Load capacitance  $C = 0.2 \text{ nF}$ .

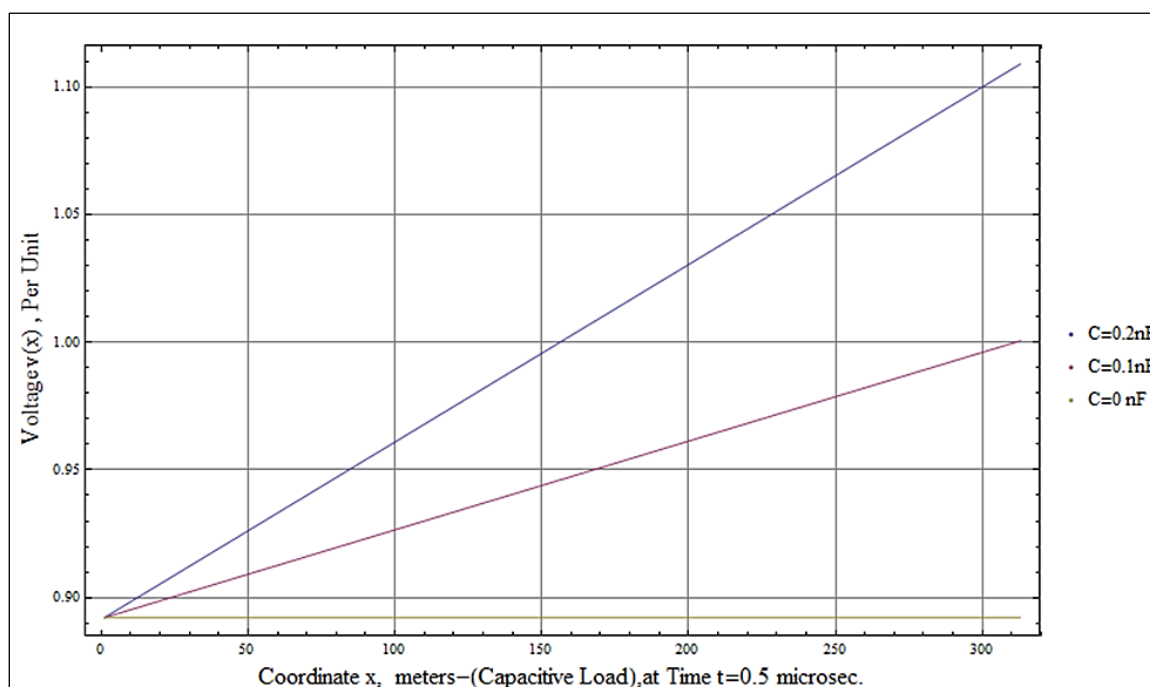


**Fig. 9:** The Voltage Distribution along the Line at  $t = 0.5 \mu\text{s}$ .

Lowest curve: Load capacitance = 0 nF,  
 Middle curve: Load capacitance = 0.1 nF,  
 Upper curve: Load capacitance = 0.2 nF.

### Impact of the Earth Conductivity $\sigma$

In order to clarify this point, two approaches will be discussed. The first one deals with the comparison of cases having different values of uniformly distributed  $\sigma$ . The second situation deals with the case of a non-uniform distribution of the earth conductivity.

#### Comparing Cases of Different but Uniformly Distributed Soil Conductivities

The three plots in Figure 10 illustrate the transient response of the receiving end voltage following the application of a unit-step source. The line is loaded by a  $0.01 \mu\text{F}$  capacitor. The plots correspond to the following values of uniformly distributed earth conductance:  $\sigma = 0.00001$ ,  $\sigma = 0.01$  and  $\sigma = 10(\Omega.\text{m})^{-1}$ . The upper curve with the least damping is for  $\sigma = 0.00001$  i.e., a highly resistive soil. It indicates a more than 50% overshoot of the receiving end voltage immediately after applying the source. The lowest curve is for a very conductive soil ( $\sigma = 10$ ) and exhibits an almost zero voltage overshoot. The intermediate curve is for  $\sigma = 0.01 (\Omega.\text{m})^{-1}$  and leads to an approximate overshoot of just 10%. The distribution of the instantaneous voltage along

the line at  $t = 5 \mu\text{sec}$  for the three values of uniform earth conductivities is described by the curves of Figure 11. Under the considered capacitive loading condition, the instantaneous voltage increases almost linearly with the distance  $x$ . The receiving end voltages assume the values 1.015, 1.0042 and 1.00 per unit for the three  $\sigma$  values 0.00001, 0.01 and 10, respectively.

#### A Case of Non-Uniformly Distributed Earth Conductivities $\sigma$

This section will demonstrate the capability of the suggested approach to dandle situations involving non-uniform earth conductivities, i.e.,  $\sigma$  is dependent on the co-ordinate  $x$ . Referring to Eq. (3), the corresponding analytical expression of  $\sigma$  will be substituted in the relation of the complex penetration depth. The following results refer to the case of a linearly decreasing  $\sigma$  (with the distance  $x$  from the line's source terminal). For simplicity, the following idealized relation is assumed:

$$\sigma(x) = a + b x \quad (14)$$

The shape of the function  $\sigma(x)$  will depend on the numerical values of the two constants  $a$



and  $b$ . For instance,  $b = 0$  represents the special case of the uniform distribution  $\sigma = a$ , whereas  $a = 0$  describes a linearly changing earth conductivity beginning with the value zero at the source terminal. The plots in Figure 12 illustrate the results for the case described by  $a = 0.1$  and  $b = -0.1/(\text{span length } d)$ .

Accordingly,  $\sigma$  has the value 0.1 at the source and decreases linearly to zero at the receiving end. Its average value is therefore,  $0.05 (\Omega \cdot \text{m})^{-1}$ . The line is loaded by a  $100 \Omega$  ohmic resistance.

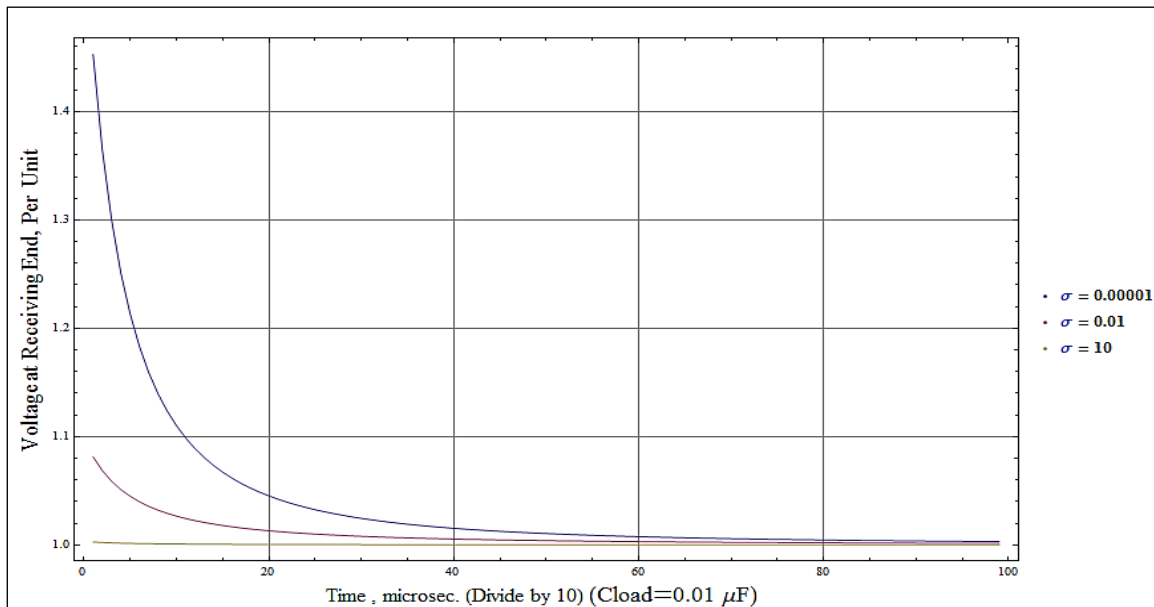


**Fig. 10:** The Transient Receiving End Voltage as affected by the Soil Conductivity  $\sigma$ . The source voltage is  $e(t) = u(t)$ .

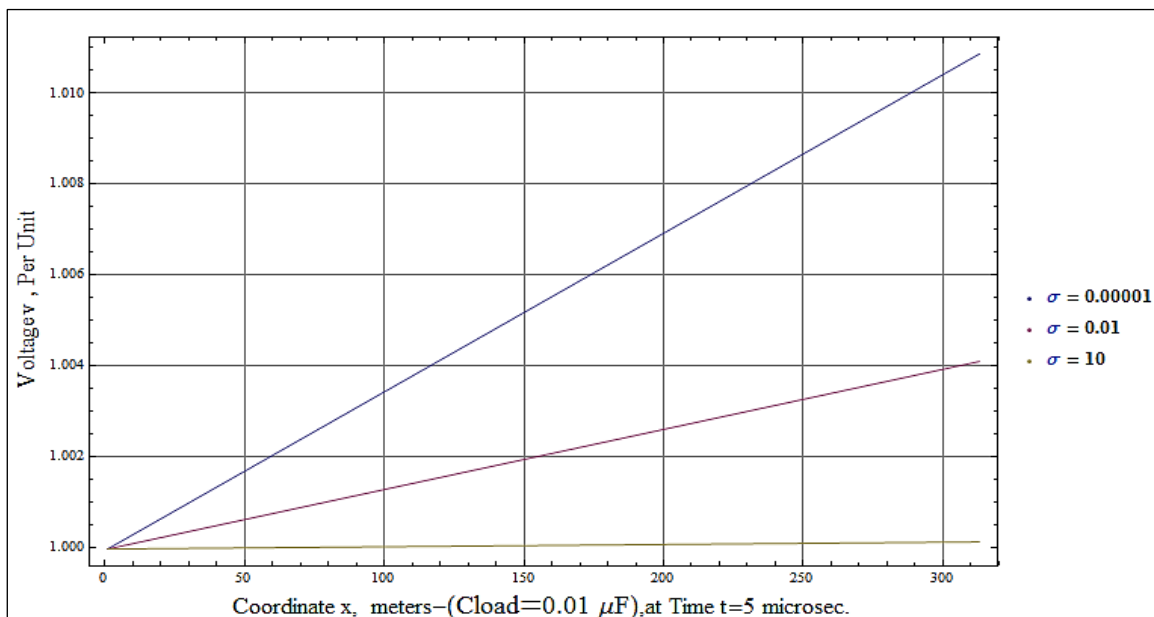


**Fig. 11:** Effect of the Soil Conductivity on the Distribution of the Transient Voltage along the Line with a Capacitive Loading of  $0.01 \mu\text{F}$  at  $t = 5 \mu\text{s}$ .

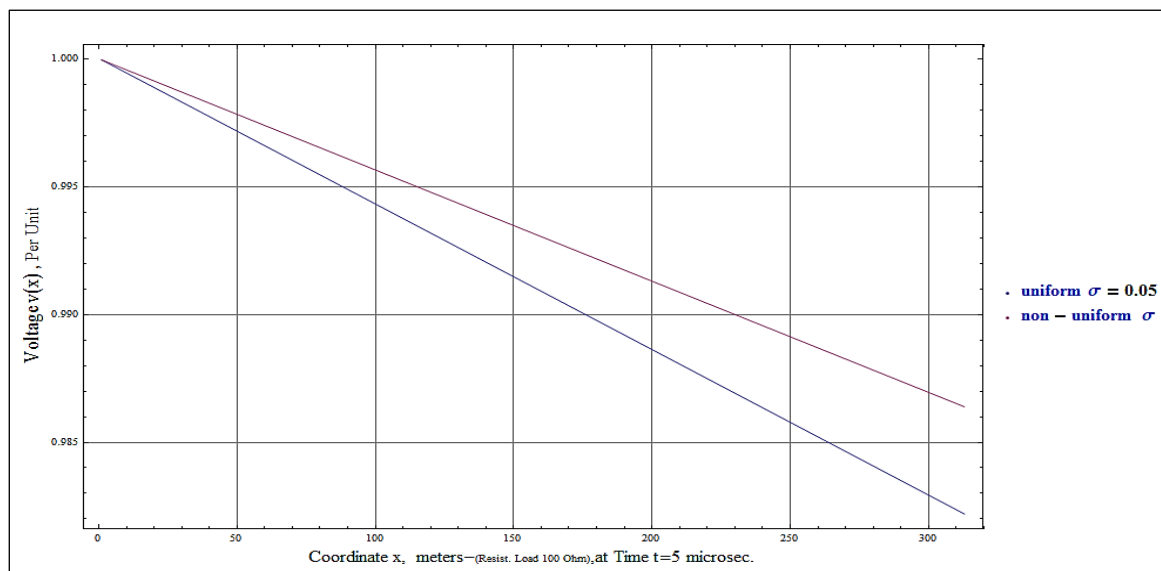


**Fig. 12:** Impact of the Non-uniformity of the Earth Conductivity on the Voltage Distribution at  $t = 5 \mu s$ .

The upper curve in Figure 12 shows the results for the above described non-uniform case. It indicates a receiving end voltage of about 0.986 per unit. This should be compared with the lower case pertinent to the case of a uniform earth conductivity  $\sigma = 0.05(\Omega \cdot m)^{-1}$ . It shows a load voltage of about 0.982 per unit. The average values of  $\sigma$  in both cases are  $0.05(\Omega \cdot m)^{-1}$ .

In principle, any other shape of non-uniformity can be similarly dealt with. Even abrupt changes in  $\sigma(x)$  can be easily expressed through the proper application of step functions.

#### Effect of the Number of Spans

Any number of span lengths can be handled by substituting the value of the number of line's tower spans  $N$  in the Eqs. (2) thru (4). As an example, Figure 13 illustrates the response of the receiving end voltage for a line comprising seven span lengths ( $N = 7$ ). The three capacitive loading conditions  $C = 0$ ,  $C = 0.1$  and  $C = 0.2$  nF previously considered in connection with Figure 8, are assumed. The expressions of the source voltage  $e(t)$  and  $E(s)$  are as given by Eqs. (11) and (12). A comparison of the plots of Figures 8 and 13 for  $N = 1$  and  $N = 7$  indicates that the receiving end voltage under no-load ( $C = 0$  nF) reaches its final value much faster if  $N = 7$ . Furthermore, the voltage overshoots in the two

other load capacitances are relatively higher for  $N = 7$ .

#### Validation of The Suggested Procedure

In order to check the validity of the suggested procedure, a special case study is selected for which an analytical solution is available. The receiving-end voltage and the source current of a lossless uniform transmission line using long line theory will be compared with those obtained from the developed *Mathematica* program using parametric functions. The results are depicted in Figure 14 for the single-span, 312.2 m long, uniform line. Its travel time is  $\tau = 1.041 \mu s$ . The conductor height is 26.2 m and its conductor radius is 0.0254 m. The wire resistance  $r_{dc}$  and its shunt conductance  $g$  are neglected in this special case study. Moreover, an infinite soil conductivity  $\sigma$  is assumed so that the complex penetration depth will be zero. A double-exponential source voltage of the following time waveform is applied:

$$e(t) = 1.034[E^{(-59523.8 t)} - E^{(-1.176 \cdot 10^7 t)}] \quad (15)$$

Its Laplace transform is

$$E(s) = \frac{1.21032 \times 10^7}{s^2 + 1.18242 \times 10^7 s + 7.0028 \times 10^{11}} \quad (16)$$

From line theory, the  $s$ -domain expressions of the voltage  $V_{RE}$  developed at the open-circuited receiving-end and the source current  $I_{Source}$  will be  $E(s)/\cosh \tau s$  and  $E(s) \tanh \tau s / Z_o$ , respectively [1].  $Z_o$  denotes the line's surge

impedance  $\sqrt{\mu_o/\epsilon_o} = 377\Omega$ . As an example, the numerical Laplace inversion the voltage expression yielded the results in plot, (a) of Figure 14. It is in good agreement with the corresponding plot, (b) obtained using the suggested procedure. The line's travel time  $\tau$

can be easily recognized from the time delay of the receiving-end voltage with respect to the applied voltage, or half the time span between any two consecutive reflections of the voltage or current waves.

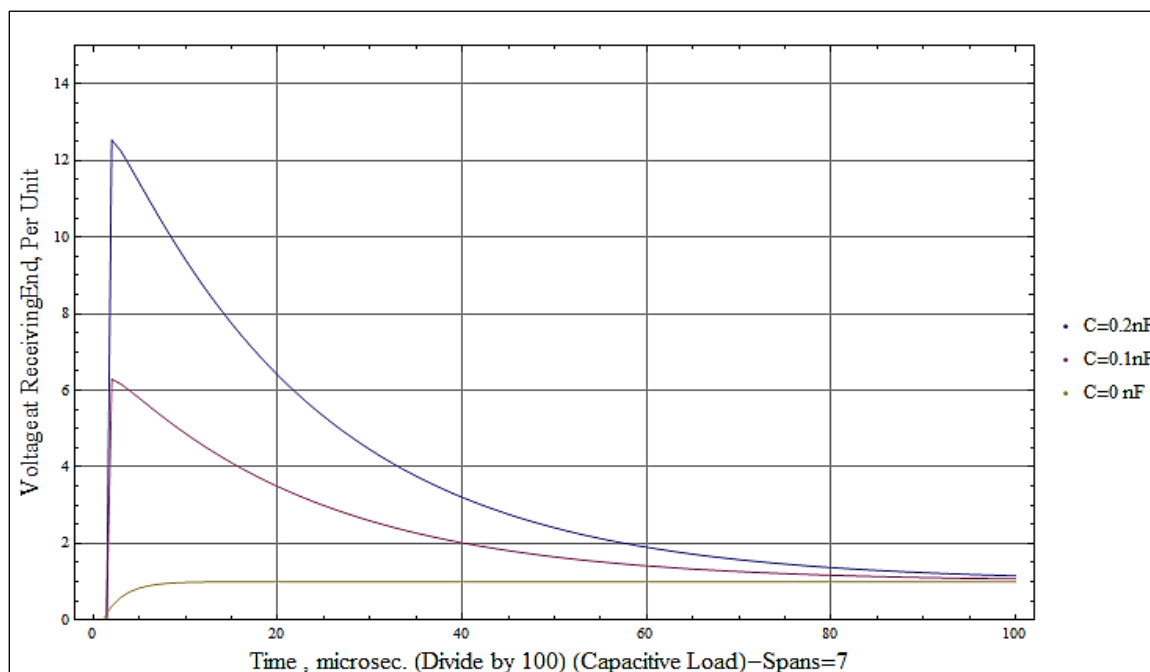
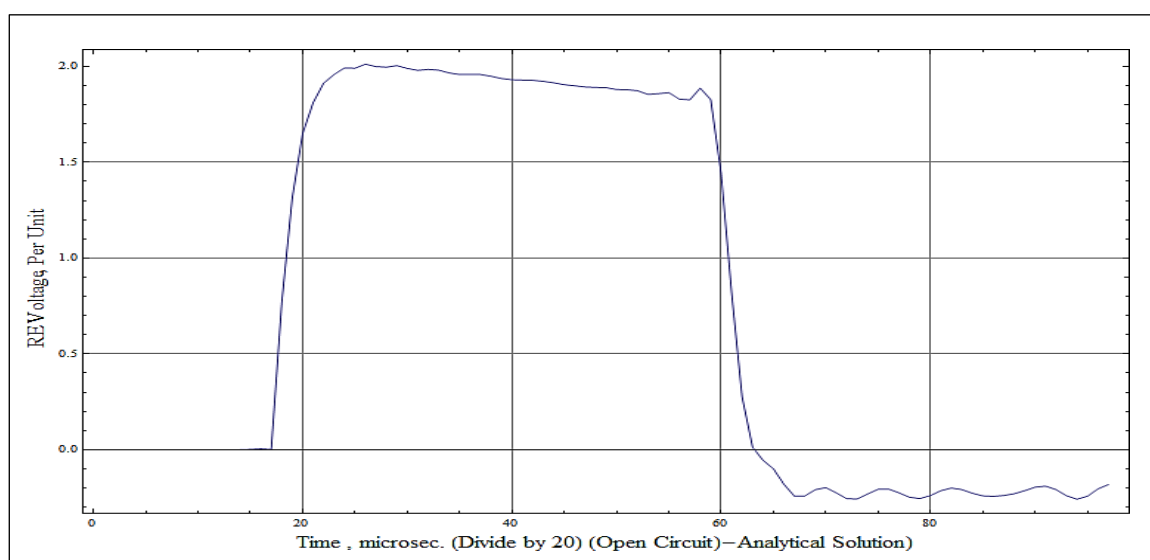
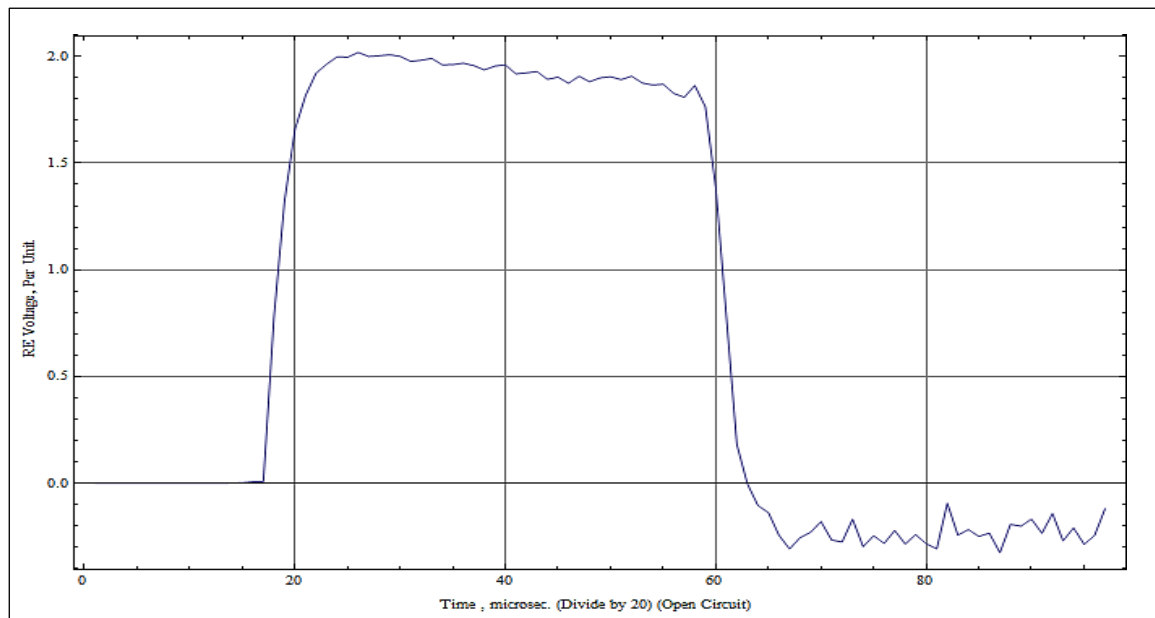


**Fig. 13:** The Transient Response of the Receiving End Voltages for Three Capacitive Loading Conditions. Number of tower spans = 7.  
 Lowest curve: Load capacitance = 0 nF,  
 Middle curve: Load capacitance = 0.1 nF,  
 Upper curve: Load capacitance = 0.2 nF.



(a) Receiving-end voltage resulting from analytical solution



(b) Receiving-End Voltage Resulting from Suggested Procedure

**Fig. 14:** Comparison of the Receiving-end Voltages Obtained using the Proposed Method and the known Analytical Solution for a Special Case Study. Time Range is:  $0 \leq t \leq 5 \mu s$ .

## CONCLUSIONS

1. A technique for analyzing the electromagnetic transients of overhead lines in the presence of conductors' sag and lossy earth return is presented.
2. A simple closed form equation expressing the conductor height as a function of the line's longitudinal co-ordinate is derived. This facilitated the formulation of the two simultaneous differential equations governing the voltage and current distributions.
3. Analytical Laplace-domain expressions for the transient voltage and current distributions in terms of the location along the line could be directly obtained using a *Mathematica* program. They were then numerically inverted into the time-domain using the Hosono algorithm.
4. The results of applying the suggested method to several case studies are presented and discussed.
5. The capability of handling situations involving soil parameters' non-uniformities, in the longitudinal direction, is pointed out.
6. The effect of the line's loading on its transient response is illustrated and discussed.
7. The suggested procedure is validated by comparing the results with those of a

certain case study with known analytical solutions using line theory.

## REFERENCES

1. Greenwood A. *Electrical Transients in Power Systems*, 2nd ed., New York: Wiley-Interscience, Chaps. 11 and 13, (1991).
2. Thrimawithana D, Madawala UK. Pulse Propagation Along Single-Wire Electric Fences, *IEEE T Power Del.* Oct. (2008); 23(4): 2302–2309p.
3. Wagner CF, Gross IW, Lloyd BL. High Voltage Impulse Tests on Transmission Lines, *Trans. AEE.* (1954); 73: 196–210.
4. Moreno P, Gómez P, Dávila M, *et al.* A Uniform Line Model for Non-Uniform Single-Phase Lines with Frequency Dependent Electrical Parameters, Paper 1-4244-0288-3/06, *Proc. IEEE PES Transmission and Distribution Conference and Exposition*, Latin America, Venezuela, (2006).
5. Alberto Gutierrez J, Jose Luis Naredo, Leonard Guardado, *et al.* Transient Analysis of Nonuniform Transmission Lines Through the Method of Characteristics, *High Voltage Engineering Symposium*, Conference Publication No. 467, O, page 1.339. P6, IEE, (1999).

6. Nelson Theethayi, Yaqing Liu, Raul Montano, *et al.* On the influence of conductor heights and lossy ground in multi-conductor transmission lines for lightning interaction studies in railway overhead traction systems, *Electr Power Syst Res.* (2004); 71: 186–193.
7. Nguyen HV, Dommel HW, Marti JR. Modeling of Single-Phase Nonuniform Transmission Lines in Electromagnetic Transient Simulations, *IEEE T Power Del.* April (1997); 12(2): 916–921p.
8. Saied MM, Al-Fuhaid AS, El-Shandwily M. s-Domain Analysis of Electromagnetic Transients on Nonuniform Lines, *IEEE T Power Del.* (1990); 5: 2072–2083p.
9. Martins TFRD, Lima ACS, Carneiro S Jr. Effect of approximate impedance formulae on the accuracy of line modeling, *IET Gener Transm. Distrib.* (2007); 1(4): 534–539p.
10. Deri A, Tevan G, Semlyen A, *et al.* The Complex Ground Return Plane. A Simplified Model for Homogeneous and Multi-Layer Earth Return. Paper No. 81 WM222-9, August 1981, *Power Engineering Review PER.* 31p, August (1981).
11. Rodolfo AR Moura, Marco AO Schroeder, Pedro HL Menezes, *et al.* Influence of the Soil and Frequency Effects to Evaluate Atmospheric Overvoltages in Overhead Transmission Lines – Part I: The Influence of the Soil in the Transmission Lines Parameters, *Proc. XV International Conference on Atmospheric Electricity*, Norman, Oklahoma, U.S.A, 15-20 June (2014).
12. Oana Simona Antonescu, Calin Munteanu, Numerical Analysis of Different Pulse Propagation on Nonuniform Transmission Lines, *2012 International Conference and Exposition on Electrical and Power Engineering (EPE 2012)*, 25-27 October, Iasi, Romania, 513–518p, (2012).
13. Saied M. A Contribution to the Frequency Analysis and Transient Response of Non-Uniform Overhead Power Lines, *Trends Electr Eng.* 3(3): (2013). Available from: ([https://www.researchgate.net/publication/260647615\\_A\\_Contribution\\_to\\_the\\_Frequency\\_Analysis\\_and\\_Transient\\_Response\\_of\\_Non-Uniform\\_Overhead\\_Power\\_Lines](https://www.researchgate.net/publication/260647615_A_Contribution_to_the_Frequency_Analysis_and_Transient_Response_of_Non-Uniform_Overhead_Power_Lines) [accessed Jul 6, 2017])
14. Leonardo Souza, Antonio Lima, Sandoval Carneiro Jr. *Modeling Overhead Transmission Line with Large Asymmetrical Spans*, *Proc. International Conference on Power Systems Transients (IPST2011) in Delft*, the Netherlands June 14-17, (2011).
15. Saied M. A Contribution to the Frequency Analysis and Transient Response of Power Transformer Windings, *J Electr Power Components Syst.* (2014); 42: 1143–1151p.
16. Hosono T. Numerical Inversion of Laplace-Transform and Some Applications to Wave Optics, *Radio Sci.* Nov. /Dec. (1981); 16(6): 1015p.

**Cite this Article**

Mohamed M. Saied. Electromagnetic Transients of a Sagging Conductor above Lossy Earth—Effect of its Loading and of the Earth Parameters. *Journal of Power Electronics & Power Systems.* 2017; 7(3): 47–59p.